M13 phage coated surface promotes anti_inflammatory responses of Balb/c peritoneal macrophages

Zohreh Safari[1], Majid Sadeghizadeh[1], Golareh Asgaritarghi[1], Hassan Bardania[2], Dina Sadeghizadeh[1], and Sara Soudi[3]

[1]Tarbiat Modares University Faculty of Biological Sciences
[2]Yasuj University of Medical Sciences
[3]Tarbiat Modares University Faculty of Medical Sciences

February 27, 2021

Abstract

The largest populations of the human virome belong to bacteriophages. M13 filamentous bacteriophages can survive, circulate and being cleared within the body. The M13 phage has been developed as a new therapeutic application due to its ability. Being detected by innate immune cells, M13 phage triggers an immune response. Hereupon, macrophages are counted as the first immune cells stimulated by phage particles. The possible interference between immune responses with the phage-induced treatment process, necessitates determining M13 phage effect on immune responses. For this purpose, M13 phage with RGD were used as substrates for macrophage culture. Gelatin and uncoated wells were used as controls. 2 and 7 days post culture on the coated surfaces, peritoneal macrophages were analyzed in terms of morphological characteristics and metabolic profile and *measurement* of cytokines production. Macrophages on M13 phage containing surfaces secreted anti-inflammatory cytokines, increased efferocytosis activity and show metabolic profile of an M2 macrophage. The results demonstrate that M13 phage can modulate immune responses by polarization of macrophages toward anti-inflammatory phenotype over time. Moreover, the combination of RGD peptide motif with M13 phage was able to stimulate macrophage polarization more effectively which may introduce an Immune-modulating technology for therapy and biocontrol.

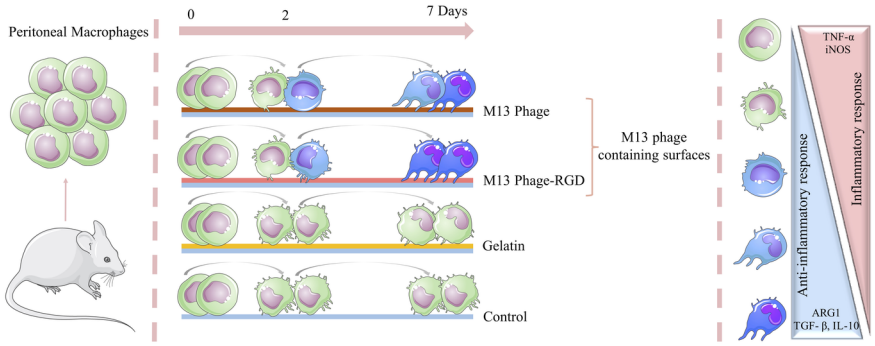

Figure 1: This is a caption

ANTI-INFLAMMATORYIMMUNO-MODULATING

Introduction:

Going beyond the primary application of bacteriophages since their discovery, phage particles as a tool have commenced to a new field of technology not only for drug delivery and drug discovery but also for therapy, biocontrol and biomedical science [1]. Although bacteriophages are bacterial viruses, they naturally come in contact with mammalian immune cells through microbiome [2]. Phages can interact with immune cells after being phagocytosis or direct contact with immune cell receptors. Both protein and nucleic acid structure of the phage can stimulate different pathogen recognition receptors of immune cells and turn on the relevant signaling pathways [3]. Moreover, phage-immune system interaction influences immune responses to environmental stimuli that leads to anti-inflammatory condition [4]. Accordingly, modulation of immune response is fundamental to regenerate multiple tissue types and in immunotherapy. Immunomodulatory drugs are usually used systemically and represent to have poor effect and being quickly lost or having toxic side effects alongside. To overcome these impediments, immunomodulatory materials can be placed at required sites to locally control immune responses[5, 6]. In recent times, biocontrol agents have been commonly used by researchers in order to control immune responses which some sort of them represent to have anti-inflammatory ability. Phages can easily be modified and include different parameters for biocontrol which can be considered as an Immunomodulatory biomaterial for therapy avoiding unwanted immune responses. [13]. It is noteworthy to mention that the formation of nanofiber structures, self-assembly, eligible size, interaction with different materials and the capability of chemical and genetic modifications of the filamentous M13 phage protein coats for expressing desired exogenous peptides have extended the application of this viral nanoparticles as a safe therapeutic tool for gene delivery, immunotherapy, tissue engineering and vaccine development[7-10]. Over and above that several researchers have illustrated the role of filamentous phages as ECM-mimicking nanofibers in enhancing cell adhesion, proliferation, and differentiation[11-13].

In the light of this notion that bacteriophages cooperate to maintain the immune homeostasis and support the immune system, [14, 15].To assess this concept, M13 phage was used as a substrate for macrophage culture and the outcome of attached macrophage responses was investigated. Macrophages was considered for the reason that they are counted as key cells in the early interaction between the material and the immune system. The characteristics of macrophages make them to have a fundamental role in the immunomodulation of the other immune cells involving in immunotherapy, drug delivery as well as regenerative process[14]The biological activity of macrophages, as crucial players in regulating immune system responses, make them mediate innate immunity and initiate responses in adaptive immunity [16-18]. One of their remarkable features is that, macrophages have functional phenotype plasticity and they react to microenvironment by changing their phenotype. As follows, they can change their polarization toward anti-inflammation (M2) or inflammation (M1) in response to microenvironment stimulus [19]. The modulation of immune responses by macrophage cells are tied to the balance of their phenotype(M1/M2)[20].Macrophages as an important source of chemokines and inflammatory molecules such as interleukin-6 and tumor necrosis factor alpha (TNF-α) are involved in initial cellular responses in inflammation occurred after immunological responses against foreign objects as delivery or implantable biomaterials utilized for therapy or tissue regeneration [21].After the initial inflammation responses, macrophage characteristics should go toward the anti-inflammatory state of the M2 macrophages, which exert their effects through the secretion of cytokines such as interleukin 10 and transforming growth factor beta (TGF- β)[22].

We hypothesize that M13 phage alter immune cell responses. It is known that the type of biomaterial exerted on macrophage cell can directly affect their phenotype and their cytokine profile[23]. The aim of the present study is to suggestion a novel application of M13 phage as an Immuno-modulating biomaterial for therapy and biocontrol. So, their bioactivity and immunostimulatory properties in encountering with macrophages were assessed in in-vitro condition. Then, the efficacy of M13 phage was measured on different macrophage immune responses including phagocytosis, efferocytosis, inflammatory and anti-inflammatory cytokine production, oxidative stress, and nitric oxide production.

Materials and methods

2.1. Large-scale amplification of M13 phage

M13 phage was grown and purified as reported previously[24, 25]. An amount of 500 mL E. coli TG1

culture was grown in 2ytx medium to mid-log phase and infected with 1 mL wild-type M13 bacteriophage (1012 PFU/ mL) was applied. The culture was incubated at 37°C with shaking for five to six hours and centrifuged at 8000g for 30 minutes to remove bacterial cells; subsequently, the virus was collected by subsequent CsCl density gradient centrifugation at 40,000 g for 2 hours. The resultant pellet was suspended in 500 μL Phosphate-buffered saline (PBS) and concentration of the isolated bacteriophage was determined spectrophotometrically using an extinction coefficient of 3.84 cm2/mg at 269 nm. This study contained 3 biological replicates (3 scaffolds of each group) and each group was replicated 3 times.

Large-scale amplification of and preparation coated surfaces

phage was grown and purified following standard biochemical protocol. An amount of 500 mL E. coli TG1 culture was grown in 2ytx media to mid-log phase and infected with 1 mL wild-type bacteriophage (10^{12} PFU/ mL). The culture was incubated at 37°C with shaking for five to six hours and centrifuged at 8000g for 30 minutes to remove bacterial cells; and then, the virus was collected by subsequent centrifuging at 20000 g for 150 minutes. The resultant pellet was suspended in 500 μL PBS and concentration of the isolated bacteriophage was determined spectrophotometrically using an extinction coefficient of 3.84 cm^2/mg at 269 nm.

Preparation of samples for TEM analysis

A solution of isolated M13 phage (20 μL) was adsorbed into a 300-mesh carbon-coated copper grid (AGS160-3) for two minutes. For transmission electron microscopy (TEM) analysis, the grid was then stained with 2% uranyl acetate. A Zeiss - EM10C - 80 KV (Oberkochen, Germany) transmission electron microscope was employed for visualizing the prepared samples.

Macrophage preparation and characterization

Twenty female BALB/c mice were obtained at six to eight weeks of age from the Pasteur Institute of Iran, and maintained in the animal laboratory in accordance with the Ethical Commission of Tarbiat Modares University guidelines. For preparation of peritoneal macrophages, 3 ml of 4% w/v thioglycollate medium was injected into the peritoneal cavity of the BALB/c mice. After four days, the macrophages were harvested by injecting; and thereafter, harvesting the fresh cold DMEM from the peritoneal cavity near the fat region of the lower abdominal area took place. Harvested peritoneal fluid was centrifuged for five minutes at 350×g and the resultant cell pellets were seeded (1×10^6 cells/ ml) to 4 or 24 well plates for downstream analysis and incubated in a humidified incubator (37@C and 5% CO2). The medium of newly isolated macrophages was changed after six hours for separating the non-adhesive cells. Phenotypic analysis of isolated cells was performed by flow cytometry for CD14+ and CD11b+ markers (Figure S2, Supporting Information) as described previously [26].

Cell viability assay

To investigate the biocompatibility of a selected concentration of M13 phage (10^{12} pfu/ml), MTT (3-(4,5-dimethylthiazol-2-yl)-2,5-diphenyltetrazolium bromide) assay was used for examining the viability of peritoneal macrophages seeded onto M13 phage, M13 phage-RGD, and gelatin-coated and control plates. Two or seven days after culture of cells in a 96 well plate (1×10^4 cells/well), MTT solution (20 μL, 5 mg/ml) was added to cell culture media and plates were incubated at 37°C. After four hours, the medium was removed and 200 μL dimethyl sulfoxide (Sigma-Aldrich, USA) was added to each well for eluting the formazan crystals, and optical density was measured at 490 nm with a microplate reader (BioTek, USA).

Morphological analysis

Macrophages were cultured on the M13 phage, M13 phage-RGD, and gelatin-coated and control 24-well plates for 2 and 7 days. Then, the cells were stained by using a PKH26 Fluorescent Cell Linker Kit (Red, Sigma-Aldrich) according to the manufacturer's recommendations. The cells were fixed with 4% paraformaldehyde

and their nuclei were stained with DAPI. Finally, fluorescently labeled macrophages were imaged with an inverted fluorescence microscope (Olympus) and analyzed by ImageJ 1.8.0.

Scanning electron microscopy

Next, the morphology of macrophages from each experimental group was observed using SEM in order to evaluate the induced morphological changes. Briefly, cells were cultured on precoated tissue culture grade coverslips and after 2 and 7 days the coverslips were air-dried. Then, the samples were gold-coated and after that they were visualized using a scanning electron microscope (KYKY-EM3200, 26KV).

RNA preparation, cDNA synthesis, and qRT-PCR

Macrophages of experimental groups were harvested for RNA extraction after two or seven days in culture. Total RNA was extracted from freshly harvested macrophages using RiboEX (GeneAll) according to the manufacturer's protocol. After Dnase treatment (Thermo), RNA samples were subjected to cDNA synthesis and qRT-PCR. RT^2 SYBR Green High ROX Master mix was used for qRT-PCR and data were quantified using [?]CT method.

Cytokine measurement

Supernatants of the macrophages in experimental groups were collected after two and seven days and stored at -20@C. The presence of IL-6, TNF-α, IL-10 and TGF- β cytokines were assessed using ELISA kits (eBioscience) following the manufacturer's instructions. Each sample was dispensed in triplicate. The optical density of each well was determined at 450 nm.

NO production

NO production was measured according to the accumulation of NO2 in culture supernatants after 2 and 7 days culture using the Griess reagent, as previously described [27]. Briefly, 100 μL of Griess reagent was mixed with equal volumes of culture supernatants from each experimental group for 10 minutes at room temperature. Then, the absorbance at 540 nm was measured using a microplate reader. Standard curve was established using a graded solution of NO2. Results were presented as mean values from three separate samples.

Determination of intracellular ROS

The accumulation of intracellular ROS in each experimental group was evaluated by using 2,7-dichlorodihydrofluorescein diacetate (DCFH-DA). This molecule de-acetylates after entry into the cells and then oxidizes with intracellular ROS to form fluorescently reactive DCF[28]. To determine ROS production, the experimental groups were incubated with DCFH-DA (10 μM) in serum-free culture media for 45 minutes at 37@C, washed twice with PBS, and finally, analyzed by flow cytometry (BD FACSCanto II, BD Bioscience, San Diego, CA, USA).

Phagocytosis assay

For phagocytosis assay, primary macrophages were seeded on M13 phage, M13 phage-RGD, and gelatin-coated and control 24 well plates; after 2 and 7 days, they were evaluated for their ability to phagocyte the labeled Saccharomyces cerevisiae (yeast) and thymus. The yeast and thymus cells were induced to apoptosis by autoclaving and UV light exposure, respectively; they were counted and stained by PI or DAPI (1mg/ml in DMEM). After staining, the cells were washed twice and resuspended in DMEM. DAPI-stained Saccharomyces cerevisiae and thymus cells were added to each well at a ratio of 5:1 (5 yeast or thymus cells:1 macrophage). Then, macrophages were incubated for one hour at 37@C and 5% CO2, and washed carefully to remove all thymus cells and yeast particles. The phagocytosis ability of macrophages in experimental

groups was detected using a flow cytometer and fluorescence microscopy after terminating the reaction with cold PBS containing 2% fetal bovine serum (FBS) and washing with PBS containing 2% paraformaldehyde.

Statistical analysis

Differences between the two experimental groups were estimated by using Student's t-test. For more than two groups, significance was estimated by using one-way analysis of variance (ANOVA). Statistical analyses were performed by a GraphPad Prism (Version 6). Data were presented as mean ± standard error of means. P ? 0.05 was considered statistically significant.

Results

Characterization of M13 bacteriophage and RGD peptide

The morphology of M13 phage was first confirmed by TEM imaging. As shown in Figure S3 (Supporting Information), TEM micrographs represent the direct observation of native M13 bacteriophage nanofilaments by diameter of 6.6 nm. Subsequently, the synthesized RGD peptide was verified by LC-MS analysis by determining the exact mass of peptide. Figure S4 (Supporting Information) shows the structure along with mass spectrum of the RGD peptide. The calculated exact mass (m/z) for peptide was reported 604.28, while the measured exact mass was 605.

Different coatings change cellular morphology and viability

To determine the effects of different coatings on cellular morphology and viability, primary mouse macrophages were placed directly on the M13, M13-RGD, and gelatin-coated and control plates. Cell morphology on each surface was observed and analyzed after two and seven days using PKH dye labeling and scanning electron microscopy (SEM) as represented in **Figure 1** A and B. According to the fluorescent microscope images and SEM micrographs, the macrophages exhibited the more pronounced outgrowth and well-spread morphology on the M13 phage containing surfaces. It should be noted that as compared to other coated surfaces, macrophages seeded on the control plates occupied the least area. Macrophages on the gelatin surface also exhibited a well-spread morphology but their cell sizes were smaller than those of M13 phage containing surfaces (**Figure 1C**). To investigate the effects of different coatings on the survival and viability of primary macrophages, cells were subjected to MTT assay on the second and seventh days. Results of MTT assay suggested that mouse macrophages in each experimental group displayed a similar viability pattern, and the survival rate was not significantly different among non-coated or coated surfaces at any point of time (**Figure 1D**).

Different surfaces alter gene expression and cytokine secretion of M1-M2 macrophage markers

In this study, to further confirm the effects of different coatings on macrophage characteristics and paracrine secretion, the gene and protein secretion of the master regulatory cytokines related to macrophage polarization were determined in both two and seven days after culture. To examine the effects of different surfaces on macrophage characteristics, we conducted qRT-PCR and ELISA assays on the second and seventh days after culture for IL-6, IL-10, TGF- β and TNF-α cytokines. Gene expression and cytokine production of IL-6 and TNF-α were upregulated in macrophages of M13 phage containing surfaces in two days; but after seven days, the expression of TNF-α showed a downtrend as compared to control surface (**Figure 2 A and B**). Accordingly, levels of IL-10 and TGF- β gene expression and cytokine secretion were much higher in M13 phage containing surfaces as compared to the control surface in both 2 and 7 days (**Figure 2C, D**). Furthermore, macrophages from gelatin surface showed the same gene expression and cytokine production patterns as control surface.

To confirm the macrophage polarization pattern, primary murine macrophages in each experimental group were either treated or not treated with LPS. 2 days later, the expression of IL-10, IL-22, CCL22, CXCL10, TNF-α, TGF- β genes were investigated. According to the results obtained, non-LPS treated macrophages cultured on M13 phage containing surfaces showed higher levels of anti-inflammatory gene expression and cytokine production as compared to gelatin and control surfaces (except for TNF-α). Interestingly, exposure

to LPS could not increase inflammatory cytokines of macrophages in M13 phage containing surfaces. (**Fig. 2E**).

Different surfaces alter gene expressions of iNOS and ARG1, NO secretion

To investigate the role of selected surfaces on polarization state of macrophages, cultured cells from each experimental group were analyzed for ARG1 and iNOS gene expression and NO secretion. Our results demonstrated that the transcript level of ARG1 in the M13 phage containing surfaces was higher than the control surface at 2 days. During the 7-day culture of cells, the gene expression of ARG1 was significantly upregulated only in the cells cultured on M13 phage-RGD surface compared to control surface (**Figure 3A**). In addition, iNOS gene expression was significantly upregulated in the M13 phage containing and Gelatin surfaces compared to their control counterparts after 2 days. While, the expression of iNOS was significantly downregulated after 7 days in M13 phage containing surfaces (**Figure 3B**). The results of qRT-PCR for iNOS gene expression were confirmed by the results of NO production in the culture supernatant of macrophages from each group (**Figure 3C**). For determining the M1/M2 balance of cultured macrophages, the ARG1/iNOS mRNA expression ratio was measured. There was a significant increase in the ratio of ARG1/iNOS mRNA in M13 phage-RGD surface compared to this ratio in control surface after 7 days cultured (**Figure 3D**).

Different surfaces alter cellular redox potential in macrophages

The redox potential of cultured macrophages was assessed using the determination of intracellular ROS production. Here, culturing of macrophages on M13 phage containing surfaces dramatically decreased the intracellular ROS level as compared to control surface in both 2 and 7 days (**Figure 4**).

Different surfaces alter phagocytosis and efferocytosis of cultured primary macrophages

To define the functional effects of selected surfaces on macrophage phagocytosis and efferocytosis, we analyzed the uptake of labeled yeasts and apoptotic cells by cultured cells. In this study, the capacity of macrophages for internalization of yeasts and apoptotic cells was evaluated by both fluorescent microscopy and flow cytometry. We found significantly increased uptake of apoptotic cells by macrophages cultured on M13 phage containing surfaces on the second and seventh days after culture. However, macrophages from control and gelatin surfaces exhibited increased level of phagocytic activity in two and seven days (**Figure 5A, B**).

Discussion:

In recent past, the importance of the biomaterial ability utilized in diverse areas including implantation, immunotherapy, drug delivery and vaccination has changed from ''immune evasive" to ''immune interactive" modulating the immune system responses in favor of mentioned biotechnological approaches [29].Bacteriophage M13 has be considered as new biomaterial for using in the regenerative processes, delivery and immunotherapy. M13 phage has specific characteristics making it to be a potential biomaterial to control the immune system responses. This filamentous bacteriophage has naturally contacted with mammalian cells. Recent studies have revealed that bacteriophages can stimulate immune cells and modulate both innate and adaptive immune responses in the host[4, 30]. Macrophages according to the environment stimulus are able to polarize into pro-inflammatory and anti-inflammatory phenotypes. Besides, they affect the other cell responses and phenotypes directly and indirectly. These abilities have made them a key regulator of immune system. Biomaterials by controlling macrophage polarization are able to mediate tolerance and modulation of the immune response[31, 32].

In the present study, we demonstrated that the M13 phage as a biomaterial is able to modulate macrophage responses. For this purpose, we examined M13 phage interaction with macrophages as a representative of tissue resident immune cells in vitro. we illustrated that M13 phage containing surfaces, change macrophage response and alter cytokine profile and polarization.

Previous reports demonstrated that RGD peptide plays a critical role in the spread of cells through focal adhesion [46]. Supporting previous studies, our immunofluorescence and scanning electron microscopy anal-

ysis represent the most dramatic increase in the cell number and contact areas of cultured macrophages on M13 phage surface and its RGD modification. Therefore, phage coated surfaces can provide better structural support for adhesion that facilitate more cell proliferation and migration[33, 34] [35]. Furthermore, our findings indicated that the M13 phage alone and the M13 phage in combination with RGD peptide are both non-toxic and biocompatible.

It has been well documented that macrophages contribute to modulate immune responses through their paracrine secretion [36]. During the early stages of normal wound healing, M1 macrophages infiltrate the wound to promote inflammation and to stimulate the wound healing process. M2 macrophages begin to accumulate around the third or fourth day after injury, while the level of M1 macrophages decreases. M2 macrophages generate in several ways including direct shift of M1 type to M2 type macrophages, polarization of newly migrating macrophages toward M2 phenotype, and proliferation of other M2 macrophages [37]. Developing a phage-based strategy modulating the host innate immune and inflammatory responses, herein, we showed that the M13 phage, especially when combined with RGD, had the ability to reprogram naive peritoneal macrophages toward M2-like phenotype. By the same token, our results demonstrated that M13 phage and RGD peptide stimulate the secretion of TNF-α, IL-6, TGF- β and IL-10 at 2 days after culture. A time-dependent increase in M2 macrophage markers (IL-10 and TGF- β [36]) and decrease in M1 macrophage marker (TNF-α [37]) was observed as well. Over and above that, cytokine analysis at both gene expression and protein level showed polarization of macrophages to M2 phenotype after interaction with M13 phage containing surfaces. Our findings indicated a significant increase in IL-6 in M13 phage containing surfaces after 2 days, while after 7 days we observed no significant changes in the level of IL-6 compared to control surface and the basal level of IL-6 remained constant after 7 days. Since IL-6 has been shown to enhance polarization of M2 macrophages [40], we postulated that the M13 phage containing surfaces could modulate the polarization of macrophages toward anti-inflammation M2 phenotype. To examine whether M13 phage containing surfaces can suppress LPS-induced inflammatory responses (LPS tolerance), we stimulated the experimental groups with LPS. Cytokine analysis demonstrated that M13 phage and RGD peptide coated surfaces polarize phenotypic characteristics similar to M2 macrophage; and also, M13 phage containing surfaces induce tolerance by inhibiting LPS-induced M2 to M1 macrophage phenotypic shift. Former investigations have adduced evidences that LPS tolerance is essential for the reduction of tissue damage and innate immune response against infection which terminated to cell proliferation and migration [41, 42].

Moreover, M2 macrophages are metabolically different from M1 macrophages and the metabolic patterns of each are directly related to their immune-modulating functions. It has been accepted that the Inducible nitric oxide synthase (iNOS) gene and NO are highly expressed in M1 macrophages, while the upregulation of arginase1 (ARG1) was observed in M2 macrophages [43].Notably, L-arginine metabolic pathway of macrophages determines the polarization status toward M1 or M2 phenotype [44]. Whilst NO is a key molecule produced by M1 macrophages to exert their role in immune defense. High level production of NO is generated from the oxidation of L-arginine. ARG1 is responsible for another metabolic pathway for L-arginine in macrophages, and this pathway produces L-ornithine for the biosynthesis of polyamine and collagen. These products help M2 macrophages to modulate biomaterial-immune system interaction [45, 46]. It is noteworthy to mention that the competition between ARG1 and NOS enzymes determine the M1/M2 phenotypic shift in macrophages. We found that the ratio of ARG1/iNOS transcript levels in the M13 phage-RGD surface was much higher than this ratio in control surface during 7 days culturing. This finding further indicated the potency of M13 phage-RGD in M2 phenotype polarization.

It has been proposed that redox potential can play a complex role in the determination of macrophage cellular fate [47]. A previous study demonstrated that ROS level is closely related to essential signaling pathways, which regulate M1 macrophage polarization [48]. It is interesting to note that interactions between ROS and NO are responsible for the regulation of cellular inflammatory conditions [49]. The decreased redox potential of macrophages on M13 phage containing surfaces in our study further emphasized the potential role of these biomaterials in reducing inflammatory responses of macrophages.

Other than that, macrophages are responsible for the clearance of microbial pathogens (phagocytosis) and apoptotic cells (efferocytosis) [50]. [48]. Likewise, alternatively activated M2 macrophages have enhanced efferocytic capability while M1 macrophages are known to have low efferocytic properties [48, 49]. Therefore, to ask if selected surfaces in the current study could alter the functional properties of macrophages, we analyzed the phagocytic and efferocytic activity of each experimental group. Our results indicated that the M13 phage containing surfaces induce macrophages to uptake the apoptotic cells, while control and gelatin surfaces lead to increased phagocytic activity by macrophages. These evidences are indicative of the fact that M13 phage and RGD peptide could functionally alter the polarization state of macrophages toward M2 phenotype.

Conclusion:

Biomaterials are most important part of strategies for biomedical technologies like drug delivery, therapy and biocontrol. Modulation of immune system and reducing inflammatory responses are one of the most important properties of immune-interactive biomaterials. Here, we demonstrated that M13 phage stimulates macrophage polarization toward anti-inflammatory phenotype, alters their cytokine profile and functional property. More interestingly, our study pointed out that the combination of well-characterized RGD peptide motif embedded in M13 phage nanostructures may enhance the macrophage responses more effectively than M13 phage surface. In conclusion, we believe that the M13 phage can be introduced as new immunomodulating biomaterial for bionanotechnological approaches.

Conflict of interest

All the Authors declare no conflict of interest.

References:

1. Twort, F.W., *An investigation on the nature of ultra-microscopic viruses.* The Lancet, 1915. **186**(4814): p. 1241-1243.

2. Reyes, A., et al., *Going viral: next-generation sequencing applied to phage populations in the human gut.* Nature Reviews Microbiology, 2012. **10**(9): p. 607-617.

3. Carroll-Portillo, A. and H.C. Lin, *Bacteriophage and the Innate Immune System: Access and Signaling.* Microorganisms, 2019. **7**(12): p. 625.

4. Van Belleghem, J.D., et al., *Interactions between bacteriophage, bacteria, and the mammalian immune system.* Viruses, 2019. **11**(1): p. 10.

5. Dellacherie, M.O., B.R. Seo, and D.J. Mooney, *Macroscale biomaterials strategies for local immunomodulation.* Nature Reviews Materials, 2019. **4**(6): p. 379-397.

6. Dziki, J.L., et al., *Extracellular matrix bioscaffolds as immunomodulatory biomaterials.* Tissue Engineering Part A, 2017. **23**(19-20): p. 1152-1159.

7. Chung, W.-J., D.-Y. Lee, and S.Y. Yoo, *Chemical modulation of M13 bacteriophage and its functional opportunities for nanomedicine.* International journal of nanomedicine, 2014. **9**: p. 5825.

8. Park, I.W., et al., *Recent Developments and Prospects of M13-Bacteriophage Based Piezoelectric Energy Harvesting Devices.* Nanomaterials, 2020. **10**(1): p. 93.

9. Avery, K.N., J.E. Schaak, and R.E. Schaak, *M13 bacteriophage as a biological scaffold for magnetically-recoverable metal nanowire catalysts: combining specific and nonspecific interactions to design multifunctional nanocomposites.* Chemistry of Materials, 2009. **21**(11): p. 2176-2178.

10. Hess, K.L. and C.M. Jewell, *Phage display as a tool for vaccine and immunotherapy development.* Bioengineering & translational medicine, 2020. **5**(1): p. e10142.

11. Wang, J., et al., *Virus activated artificial ECM induces the osteoblastic differentiation of mesenchymal stem cells without osteogenic supplements.* Scientific reports, 2013. **3**: p. 1242.

12. Wang, J., et al., *Phage nanofibers induce vascularized osteogenesis in 3D printed bone scaffolds.* Advanced Materials, 2014. **26**(29): p. 4961-4966.

13. Merzlyak, A., S. Indrakanti, and S.-W. Lee, *Genetically engineered nanofiber-like viruses for tissue regenerating materials.* Nano letters, 2009. **9**(2): p. 846-852.

14. Górski, A., et al., *Phages and immunomodulation.* Future microbiology, 2017. **12**(10): p. 905-914.

15. Lai, Y.S., et al., *Autocrine VEGF signalling on M2 macrophages regulates PD-L1 expression for immunomodulation of T cells.* Journal of cellular and molecular medicine, 2019. **23**(2): p. 1257-1267.

16. Wynn, T.A., A. Chawla, and J.W. Pollard, *Macrophage biology in development, homeostasis and disease.* Nature, 2013. **496**(7446): p. 445.

17. Gurtner, G.C., et al., *Wound repair and regeneration.* Nature, 2008. **453**(7193): p. 314.

18. Zhou, G. and T. Groth, *Host Responses to Biomaterials and Anti-Inflammatory Design—a Brief Review.* Macromolecular bioscience, 2018. **18**(8): p. 1800112.

19. Mosser, D.M. and J.P. Edwards, *Exploring the full spectrum of macrophage activation.* Nature reviews immunology, 2008. **8**(12): p. 958-969.

20. Wang, N., H. Liang, and K. Zen, *Molecular mechanisms that influence the macrophage M1–M2 polarization balance.* Frontiers in immunology, 2014. **5**: p. 614.

21. Chung, L., et al., *Key players in the immune response to biomaterial scaffolds for regenerative medicine.* Advanced drug delivery reviews, 2017. **114**: p. 184-192.

22. Wynn, T.A. and K.M. Vannella, *Macrophages in tissue repair, regeneration, and fibrosis.* Immunity, 2016. **44**(3): p. 450-462.

23. Badylak, S.F., et al., *Macrophage phenotype as a determinant of biologic scaffold remodeling.* Tissue Engineering Part A, 2008. **14**(11): p. 1835-1842.

24. Reddy, P. and K. McKenney, *Improved method for the production of M13 phage and single-stranded DNA for DNA sequencing.* Biotechniques, 1996. **20**(5): p. 854-860.

25. Nasukawa, T., et al., *Virus purification by CsCl density gradient using general centrifugation.* Archives of virology, 2017. **162**(11): p. 3523-3528.

26. Goncalves, R. and D.M. Mosser, *The isolation and characterization of murine macrophages.* Current protocols in immunology, 2015: p. 14.1. 1-14.1. 16.

27. Edwards, J.P., et al., *Biochemical and functional characterization of three activated macrophage populations.* Journal of leukocyte biology, 2006. **80**(6): p. 1298-1307.

28. Eruslanov, E. and S. Kusmartsev, *Identification of ROS using oxidized DCFDA and flow-cytometry*, in *Advanced protocols in oxidative stress II*. 2010, Springer. p. 57-72.

29. Vishwakarma, A., et al., *Engineering immunomodulatory biomaterials to tune the inflammatory response.* Trends in biotechnology, 2016. **34**(6): p. 470-482.

30. Sinha, A. and C.F. Maurice, *Bacteriophages: uncharacterized and dynamic regulators of the immune system.* Mediators of inflammation, 2019. **2019**.

31. Yang, H.-C., et al., *Immunomodulation of Biomaterials by Controlling Macrophage Polarization*, in *Biomimetic Medical Materials*. 2018, Springer. p. 197-206.

32. Sridharan, R., et al., *Biomaterial based modulation of macrophage polarization: a review and suggested design principles.* Materials Today, 2015. **18**(6): p. 313-325.

33. Yang, D., et al., *Promoting cell migration in tissue engineering scaffolds with graded channels.* Advanced healthcare materials, 2017. **6**(18): p. 1700472.

34. Li, X., et al., *Induced migration of endothelial cells into 3D scaffolds by chemoattractants secreted by pro-inflammatory macrophages in situ.* Regenerative biomaterials, 2017. **4**(3): p. 139-148.

35. Richbourg, N.R., N.A. Peppas, and V.I. Sikavitsas, *Tuning the Biomimetic Behavior of Scaffolds for Regenerative Medicine Through Surface Modifications.* Journal of tissue engineering and regenerative medicine, 2019.

36. Corliss, B.A., et al., *Macrophages: an inflammatory link between angiogenesis and lymphangiogenesis.* Microcirculation, 2016. **23**(2): p. 95-121.

37. Yu, T., V.J. Tutwiler, and K. Spiller, *The role of macrophages in the foreign body response to implanted biomaterials*, in *Biomaterials in Regenerative Medicine and the Immune System.* 2015, Springer. p. 17-34.

38. Makita, N., et al., *IL-10 enhances the phenotype of M2 macrophages induced by IL-4 and confers the ability to increase eosinophil migration.* International Immunology, 2015. **27**(3): p. 131-141.

39. Shapouri-Moghaddam, A., et al., *Macrophage plasticity, polarization, and function in health and disease.* Journal of cellular physiology, 2018. **233**(9): p. 6425-6440.

40. Fernando, M.R., et al., *The pro-inflammatory cytokine, interleukin-6, enhances the polarization of alternatively activated macrophages.* PLoS One, 2014. **9**(4): p. e94188.

41. Foey, A.D. and S. Crean, *Macrophage subset sensitivity to endotoxin tolerisation by Porphyromonas gingivalis.* PLoS One, 2013. **8**(7): p. e67955.

42. O'Carroll, C., et al., *Identification of a unique hybrid macrophage-polarization state following recovery from lipopolysaccharide tolerance.* The Journal of Immunology, 2014. **192**(1): p. 427-436.

43. Jin, Y., Y. Liu, and L.D. Nelin, *Extracellular signal-regulated kinase mediates expression of arginase II but not inducible nitric-oxide synthase in lipopolysaccharide-stimulated macrophages.* J Biol Chem, 2015. **290**(4): p. 2099-111.

44. Rath, M., et al., *Metabolism via arginase or nitric oxide synthase: two competing arginine pathways in macrophages.* Frontiers in immunology, 2014. **5**: p. 532.

45. Li, Z., et al., *Differences in iNOS and arginase expression and activity in the macrophages of rats are responsible for the resistance against T. gondii infection.* PloS one, 2012. **7**(4): p. e35834.

46. Rőszer, T., *Understanding the mysterious M2 macrophage through activation markers and effector mechanisms.* Mediators of inflammation, 2015. **2015**.

47. Tan, H.-Y., et al., *The reactive oxygen species in macrophage polarization: reflecting its dual role in progression and treatment of human diseases.* Oxidative medicine and cellular longevity, 2016. **2016**: p. e2795090.

48. Lee, A.S., et al., *SIRT2 ameliorates lipopolysaccharide-induced inflammation in macrophages.* Biochemical and biophysical research communications, 2014. **450**(4): p. 1363-1369.

49. McNeill, E., et al., *Regulation of iNOS function and cellular redox state by macrophage Gch1 reveals specific requirements for tetrahydrobiopterin in NRF2 activation.* Free Radic Biol Med, 2015. **79**: p. 206-16.

50. Korns, D.R., et al., *Modulation of macrophage efferocytosis in inflammation.* Frontiers in immunology, 2011. **2**: p. 57.

51. Sun, L., et al., *Ex vivo and in vitro effect of serum amyloid a in the induction of macrophage M2 markers and efferocytosis of apoptotic neutrophils.* The Journal of Immunology, 2015. **194**(10): p. 4891-4900.

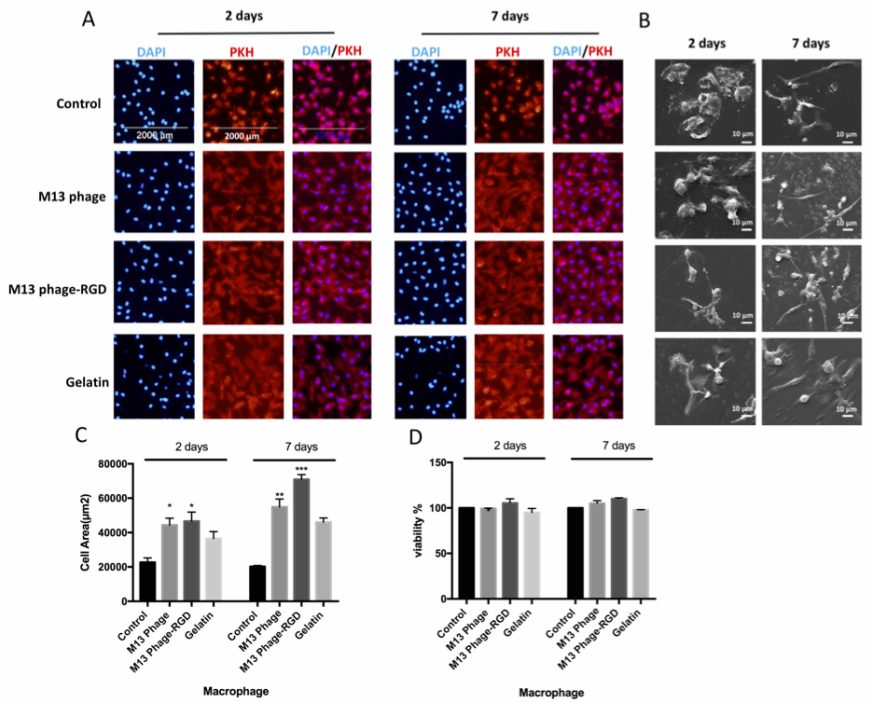

Figure 2: **Figure 1:** Outgrown morphology of Macrophage stimulated by Phage-RGD tissue matrices. (A) Fluorescent microscopy images of outgrown Macrophage after 2 and 7 days culture. The cells are stained by PKH (red), DAPI (blue) (B) representative scanning electronic micrographs images of the macrophages on different surfaces at 2 and 7 days (C) Quantification of the cell areas on m13 phage, m13 phage-RGD and gelatin film and control after 2 and 7 days culture. Two to three fields of views were taken to analyze each image (cell n = 3-6 per one field of view, (D) MTT cell proliferation assays on different types of film. MTT assay result shows that cells all groups have a similar viability pattern (*; Significant at P-value<0.05, **; Significant at P-value<0.01, ***; Significant at P-value<0.001). (scale bar = 2000 µm).

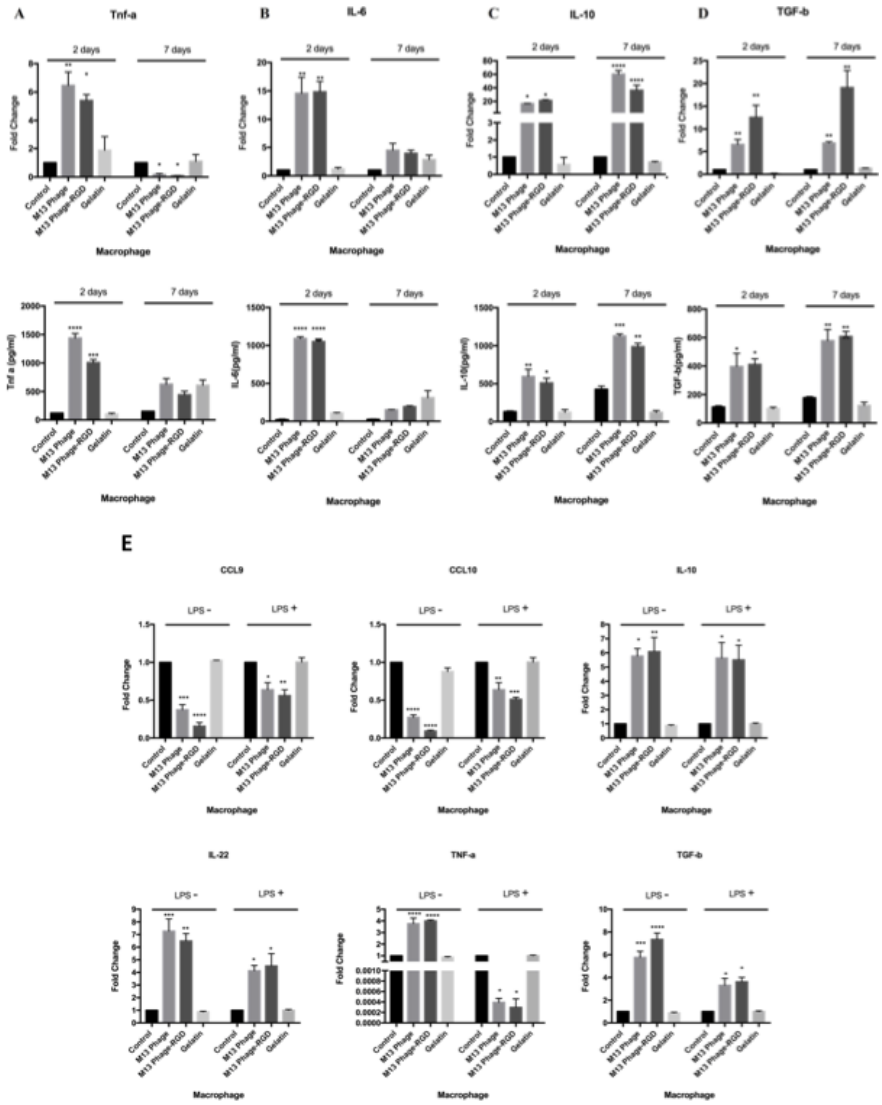

Figure 3: This is a caption

Figure 2: quantitative analysis. (A-D) quantitative analysis of IL-10, IL-6, Tnf- α transcript levels and Secretion of IL-10, Tnf- α and IL-6 in macrophage on four surfaces after 2 and 7 days.

(E) quantitative analysis of CXCL9, CXCL10, IL-10, IL-22, Tnf- α, TGF- β in macrophages after culture on each surface in the absence or presence of LPS for 2 days.

Value for genes mRNA expression were normalized to GAPDH mRNA levels for each experimental condition. (*; Significant at P-value<0.05, **; Significant at P-value<0.01, ***; Significant at P-value<0.001) (n=3)

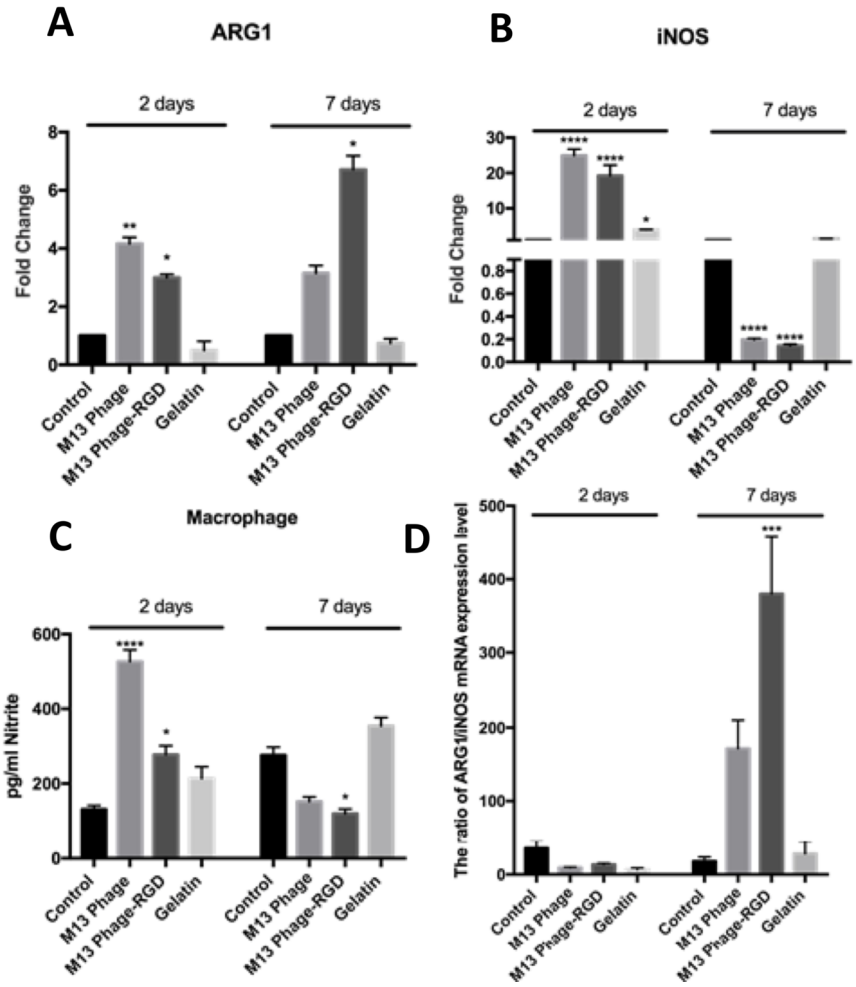

Figure 4: **Figure 3:** iNOS and ARG1 expression, nitric oxide (NO) production in peritoneal macrophages from 4 groups experimental. (A) Amplicons densitometrically quantified; bars represent the relative amounts of amplified arginase-1 mRNA normalized against GAPDH, RT-PCR analysis for the expression of arginase-1 mRNA. (B) Amplicons were densitometrically quantified; bars represent relative amounts of amplified iNOS mRNA normalized against GAPDH. (C)Comparison of NO production, in macrophages at 2 and 7 days. (D) Comparison of levels of expression of iNOS with ARG1 mRNAs at 2 and 7 days. Graph shows collective data (*; Significant at P-value$<$0.05, **; Significant at P-value$<$0.01, ***; Significant at P-value$<$0.001). (n=3)

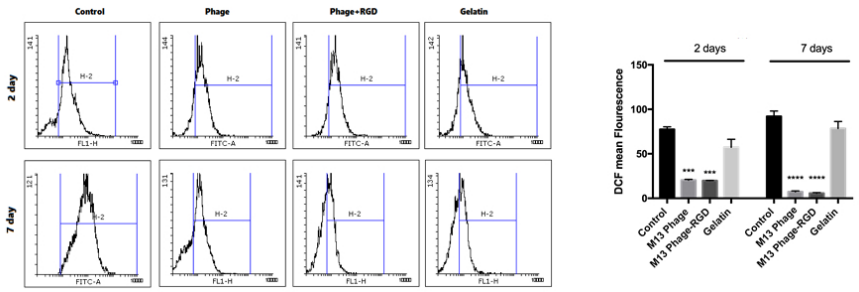

Figure 5: **Figure 4:** intracellular ROS level in peritoneal macrophages from 4 groups surfaces. The effect of different surfaces on the intracellular ROS level was determined by flow cytometry analysis at 2 and 7 days. Graph shows collective data (*; Significant at P-value<0.05, **; Significant at P-value<0.01, ***; Significant at P-value<0.001). (n=3)

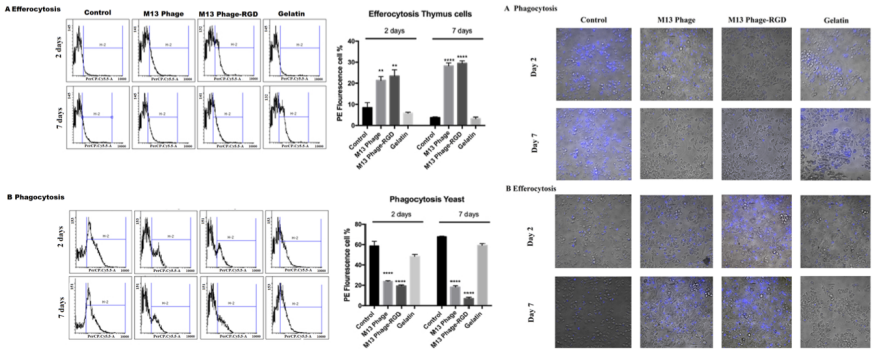

Figure 6: This is a caption

Figure 5: Flow cytometric analyses of phagocytosis and efferocytosis. Unstained macrophage cells culture on control, M13phage, M13phage-RGD and gelatin surfaces for 2 and 7 days after co-cultured for 1 hours with stained yeast (PE-red) or stained apoptotic cells (PE-red) and fluorescence images of analyses of phagocytosis and efferocytosis. Unstained macrophage cells culture on control, M13phage, M13phage-RGD and gelatin surfaces for 2 and 7 days after co-cultured for 1 hours with stained yeast (DAPI-blue) or stained apoptotic cells (DAPI-blue).

(A) Flow cytometric and fluorescence images analyses of macrophages efferocytosis. Representative histogram shows the macrophage marker PE indicating efferocytosis.

(B) Flow cytometric fluorescence images analyses of macrophages phagocytosis. Representative histogram shows the macrophage marker PE indicating Phagocytosis.